The Carboxyl Side Chain of Glutamate 681 Interacts with a Chloride Binding Modifier Site That Allosterically Modulates the Dimeric Conformational State of Band 3 (AE1). Implications for the Mechanism of Anion/Proton Cotransport†

James M. Salhany,*,‡,§ Renee L. Sloan,‡ and Karen S. Cordes‡

Veterans Administration Medical Center, 4101 Woolworth Avenue, Omaha, Nebraska 68105, and Department of Internal Medicine and Department of Biochemistry and Molecular Biology, University of Nebraska Medical Center, Omaha, Nebraska 68198-5290

Received August 13, 2002; Revised Manuscript Received November 19, 2002

ABSTRACT: Glutamate 681 is thought to be located within the transport channel of band 3 (AE1, the chloride/bicarbonate exchanger), where it acts as a proton donor for the anion/proton cotransport function. Here we show that neutralization of the negative charge on glutamate 681 by chemically modifying band 3 with Woodward's reagent K plus sodium borohydride (i.e., the modification process) exposes a cryptic, conformationally active chloride-binding site which functions to modulate allosterically the conformational state of the band 3 dimer. Chloride binding was determined by measuring the effect of increasing chloride concentration on the rate of DBDS (4,4′-dibenzamido-2,2′-stilbenedisulfonate) release from band 3 using a stopped-flow fluorescence kinetic inhibitor replacement assay with DIDS (4,4′-diisothiocyanato-2,2′-stilbenedisulfonate) as the replacing inhibitor. The time course for DBDS release from unmodified, control band 3 was monophasic and exponential. Chloride binding to the transport site accelerated the rate of DBDS release, with the observed rate constant showing a hyperbolic dependence on chloride concentration, while the total change in reaction fluorescence remained constant. After modification of glutamate 681, DBDS release was monophasic in the absence of chloride, but the rapid addition of chloride at constant ionic strength induced a doubling in the fluorescence quantum yield for the bound DBDS molecules. This was associated with the development of 50:50 biphasic kinetics for DBDS release. Such changes were independent of the degree of modification of the band 3 subunit population between the 66% and 91% levels. Titration of the increase in total reaction fluorescence gave an apparent chloride binding K_d of between 7 and 10 mM, which is 25−40-fold higher in affinity than chloride binding to the transport site. The dependence of the kinetic constants for both phases of the DBDS release reaction on chloride concentration was nonhyperbolic, which contrasts with unmodified band 3, and is indicative of the presence of two classes of chloride-binding sites on the modified transporter. We have also found that the fraction of subunits capable of binding DBDS reversibly, or DIDS covalently, decreased nonlinearly in the absence of chloride as the level of modification of the band 3 subunit population increased. In contrast, the same DBDS binding correlation plot showed a maximum in the presence of saturating chloride. The observation of such nonlinear correlation plots is consistent with a noncooperative dimer model for the modification process, where each dimeric species must possess different properties with respect to stilbenedisulfonate binding capacity and with respect to the spectral−kinetic response of bound stilbenedisulfonate molecules to the addition of chloride. Within the context of this model, the fractions of the three molecular dimeric species (i.e., the unmodified dimer, the dimer with one subunit modified, and the fully modified band 3 dimer) are calculated as a function of the level of modification of the band 3 subunit population. Nonlinear correlation plots are generated by then assigning the following specific properties to each dimeric species. The unmodified dimer binds DBDS but does not change its fluorescence quantum yield upon addition of chloride. The half-modified dimer binds DBDS on both modified and unmodified subunits, and both of those DBDS molecules increase their fluorescence quantum yield by 2-fold when chloride is added, and the system develops 50:50 biphasic DBDS release kinetics. Finally, the model requires that the fully modified dimer does not bind DBDS or DIDS. This model generates theoretical correlation plots that can represent the data presented in this study. We propose that neutralization of glutamate 681 on the half-modified band 3 dimer exposes an allosteric, chloride-binding modifier site which functions to facilitate the anion/proton cotransport process (a) by blocking the "redocking" of the carboxyl side chain of glutamate (thus raising its p*K*) and (b) by inducing a conformational change in the band 3 dimer from a symmetrical to an asymmetrical state.

The primary physiological function of band 3 (AE1) is to exchange chloride for bicarbonate across the human erythrocyte membrane (*1*−*4*). However, band 3 can also transport divalent anions but with significantly different characteristics (*1*−*3*). One major difference is seen when the extracellular pH is lowered from 7.0 to 5.0. This change inhibits rapid monovalent anion exchange (*5*, *6*) but accelerates sulfate influx into chloride-loaded cells (*7*, *8*). Gunn (*9*) proposed a "titratable carrier" model in an attempt to rationalize such different characteristics. The model suggests that a "carrier" for monovalent anions can be converted to a carrier for divalent anions by protonation. Thus, the monova-

† This work was supported by a Merit Review Grant from the Medical Research Service of the Veterans Administration.

* To whom correspondence should be addressed at the Department of Internal Medicine, University of Nebraska Medical Center. Phone: (402) 559-6281. Fax: (402) 559-6309. E-mail: jsalhan@attglobal.net.

‡ Veterans Administration Medical Center.

§ University of Nebraska Medical Center.

10.1021/bi0205294 CCC: $25.00
Published on Web 01/21/2003

lent form of the carrier binds a proton and a divalent anion, allowing for their cotransport in exchange for chloride. One manifestation of such a cotransport function for band 3 is that at low pH, where band 3-mediated chloride self-exchange is nearly zero (*5*), it may be possible for band 3 to cotransport chloride and a proton (*10*). Passow and co-workers (*11*) have presented evidence suggesting that proton transport at low pH may involve two chloride-binding sites.

The observed p*K* (~5.9 at 22 °C) (*8*) for the conversion of band 3 from the monovalent anion-exchange state to the anion/proton cotransport functional state suggested that a carboxyl side chain may be involved (*3*). Jennings and Al-Rhaiyel (*12*) presented evidence supporting this suggestion by showing that modification of band 3 by treatment of intact erythrocytes with Woodward's reagent K (WRK)[1] and sodium borohydride (herein called the modification process or, simply, modification of band 3) could mimic protonation of band 3. Modification of band 3 involves neutralization of the charge on the carboxyl side chain of glutamate residues by converting them to an alcohol (*12*). Jennings and Smith (*13*) then showed that the method of Jennings and Al-Rhaiyel (*12*) modifies glutamate 681 of band 3 and that no other glutamate residue was detectably modified under the conditions of their experiments. They demonstrated this specificity using a radiolabeling method with Edman degradation of the major proteolytic fragments of band 3. It was concluded that glutamate 681 is the binding site for the proton that is transported with sulfate during band 3-mediated sulfate/proton cotransport. The functional characteristics of this residue suggested that it lies within the transport pathway and that it can be exposed, alternately, to the intracellular and extracellular media (*12*). Recent site-directed mutation studies involving studies of substitutions at the position of glutamate 681 have supported the assignment of this residue to the anion/proton cotransport function (*14*, *15*).

At present, it is not clear how protonation of glutamate 681 causes interconversion of band 3 between the monovalent and divalent anion transport functional states. Some insight into the relationship between anion-exchange and anion/proton cotransport mechanisms may be gained by considering the recent X-ray crystal structural studies of a bacterial ClC chloride channel (*16*). The chloride-binding sites in this channel are formed by partial charges from backbone amide nitrogens and the side chains of tyrosine and serine, as well by several hydrophobic residues, rather than by direct interaction with arginine or lysine side chains. Interestingly, it was found that a glutamate residue blocked access of chloride to the external aqueous region of the channel. Dutzler et al. (*16*) suggested that this residue may act as a gate. This gate opens when chloride induces a conformational change by competing with and displacing the glutamate side chain from its binding site. Since glutamate 681 is thought to be located at a diffusion barrier within the transport channel of band 3 (*13*), we hypothesized that it may interact with a conformationally active chloride-binding modifier site, which is distinct from the transport site. This proposal would be consistent with the work of Passow and co-workers (*11*), suggesting that two chloride-binding sites may be involved in chloride/proton cotransport process at low pH.

We tested the modifier site hypothesis by using the Woodward's reagent K/sodium borohydride treatment method of Jennings and Al-Rhaiyel (*12*) to neutralize the side chain of glutamate 681 (*13*) to see if a second chloride-binding site could be detected. Earlier chloride NMR studies of chloride binding did not demonstrate the presence of two chloride-binding sites after band 3 was treated with Woodward's reagent K (*17*). However, those studies were performed without treatment with sodium borohydride to remove the Woodward's reagent K covalent adduct.

We used a stopped-flow fluorescence kinetic method established in our laboratory (*18*) to measure chloride binding to band 3. This method exploits the chloride sensitivity of the kinetics of release of DBDS from a preexisting binary complex with band 3 (*18*−*21*). The time course for the release reaction follows single exponential kinetics. Secondary plots of the observed rate constant versus chloride concentration are always hyperbolic (*18*). The site responsible for this effect was demonstrated to be the chloride-binding transport site (*19*). Here we describe both fluorescence and kinetic changes induced in bound DBDS molecules by addition of chloride to erythrocyte membranes derived from intact erythrocytes treated with the Woodward's reagent K/sodium borohydride modification process, which specifically neutralizes glutamate 681 (*13*).

EXPERIMENTAL PROCEDURES

Materials

Erythrocytes were obtained from the Omaha Chapter of the American Red Cross. WRK, DIDS, and the various buffers used in this study were all obtained from Sigma. DBDS was synthesized as described previously (*18*), or it was obtained from Molecular Probes (Eugene, OR). Other chemicals were of reagent grade.

Methods

Summary of Procedures Used To Modify Glutamate 681. We used the method of Jennings and Al-Rhaiyel (*12*) to modify band 3 subunits. We treated intact erythrocytes with constant WRK (2 mM) in one treatment cycle and then added sodium borohydride (called WRKB), or we performed two such treatment cycles [called 2(WRKB)]. To modify additional band 3 subunits, we used a variation of the method described by Jennings (*22*), where cells were treated with 2 mM WRK twice and then treated with sodium borohydride [called (2WRK + B)]. Lower levels of modification of the subunit population of band 3 were generated as described for WRKB, except that lower concentrations of WRK were used (*12*). The specific details for each treatment strategy used in this study are described below. Prior to those various treatments, erythrocytes were washed four times in PBS (150 mM sodium chloride, 5 mM sodium phosphate, pH 8) to remove plasma and buffy coat and then three times in the KCl/MOPS reaction buffer (150 mM KCl, 10 mM MOPS, pH 7.0).

[1] Abbreviations: Woodward's reagent K (WRK), *N*-ethyl-5-phenylisoxazolium-3′-sulfonate; WRKB, Woodward's reagent K treatment followed by treatment with sodium borohydride; DIDS, 4,4′-diisothiocyanato-2,2′-stilbenedisulfonate; DBDS, 4,4′-dibenzamido-2,2′-stilbenedisulfonate; H_2DIDS, 4,4′-diisothiocyanatodihydro-2,2′-stilbenedisulfonate; MOPS, 3-(*N*-morpholino)propanesulfonic acid; Bistris, *N*,*N*-[bis(2-hydroxyethyl)amino]tris(hydroxyaminoethyl)aminomethane; Tris, tris(hydroxymethyl)aminomethane.

Specific Procedures Used To Modify Glutamate 681. (A) WRKB Treatment. Twenty milliliters of washed, packed erythrocytes was suspended up to 200 mL in the KCl/MOPS buffer (10% final hematocrit) and chilled in ice water to less than 2 °C. Solid WRK was added to this suspension to give a final concentration of 2 mM. In some experiments, 0.5 mM WRK or 1 mM WRK was used. This mixture was allowed to stand for 10 min at 2 °C, after which sodium borohydride was added from a 1 M stock solution to a final concentration of 2 mM. This mixture was allowed to stand for 5 min at 2 °C, after which MOPS acid was added from a 1 M stock solution to yield 10 mM. A second addition of sodium borohydride was added immediately to a final concentration of 2 mM. This suspension was allowed to stand for 5 min at 2 °C, after which the cells were washed two times in the KCl/MOPS buffer. A portion of the cells was saved for the transport assays described below, while the remainder was used to make unsealed ghosts as described elsewhere (*18*).

(B) 2(WRKB) Treatment. Cells were treated twice exactly as just described for the 2 mM WRKB reaction. The second full cycle was performed with a freshly made 1 M stock solution of sodium borohydride. A portion of this sample was taken for transport, and the remainder was used to make unsealed ghosts.

(C) (2WRK + B) Treatment. Twenty milliliters of washed, packed erythrocytes was suspended up to 200 mL in the KCl/MOPS buffer (10% final hematocrit) and chilled in ice water to less than 2 °C. Solid WRK was added to this suspension to give a final concentration of 2 mM. Cells were allowed to stand for 20 min at 2 °C, after which they were washed two times in the KCl/MOPS buffer. The cells were then resuspended to a 10% hematocrit in the KCl/MOPS buffer to which solid WRK was added again to 2 mM final concentration. This suspension was allowed to stand at 2 °C for 10 min, after which sodium borohydride was added to 2 mM from a 1 M stock solution. This suspension was allowed to stand for 5 min at 2 °C, after which MOPS acid was added to 10 mM final concentration from a 1 M stock solution. This was followed immediately by a second addition of sodium borohydride to 2 mM. This suspension was allowed to stand for 5 min at 2 °C, after which it was washed twice in the KCl/MOPS buffer. A portion of this sample was taken for transport, and the remainder was used to make unsealed ghosts.

Prelabeling of Intact Erythrocytes with DIDS. Prelabeling of erythrocytes was accomplished as described earlier (*18*). PBS-washed erythrocytes were incubated with various concentrations of DIDS at 50% hematocrit for 45 min at 37 °C. After incubation the cells were washed in PBS plus 5% bovine serum albumin and then two more times in PBS to remove unreacted DIDS. A portion of these cells was used for transport, while the remainder was used to make unsealed ghosts as described earlier (*18*).

Thiocyanate/Chloride Exchange. We used a spectrophotometric method described earlier (*23*) to measure this monovalent hetero-anion-exchange process using intact erythrocytes at 25 °C. The reaction was initiated by mixing cells (1% hematocrit) in 150 mM KCl and 10 mM MOPS, pH 7.0, 50:50 in the stopped-flow apparatus, with 150 mM sodium thiocyanate in the same buffer. Initial rates were determined from semilog plots of the time courses (*23*). The percent inhibition was calculated as $100[1 - (k_i/k_0)]$, where k_0 is the initial rate constant for unmodified, control erythrocytes.

Covalent Binding of DIDS to "Lysine A" of Band 3. This reaction was monitored using a fluorometric method described earlier (*24*). Unsealed ghosts were derived from the same erythrocytes prepared as described above and suspended in 300 mM sodium gluconate and 20 mM Bistris, plus 20 mM Tris, pH 7.4. The total protein for each membrane sample was measured and matched as described previously (*25*), so that the amount of band 3 in each sample was the same. Each sample was mixed in the stopped-flow apparatus with a DIDS solution (13 μM) prepared in the above gluconate buffer. The reaction was followed by exciting the mixture at 360 nm and following the increase in fluorescence associated with covalent bond formation (*24*) through a 415 nm cutoff filter. The percent of DIDS adduct formation was determined by measuring ΔF_{total} by following each reaction to completion and dividing each experimental ΔF_{total} by ΔF_{total} for the unmodified control and multiplying by 100.

Dithionite/Chloride Exchange. The reactions were measured in the stopped-flow apparatus as described earlier (*26*, *27*). Cells (2% hematocrit) in 150 mM KCl and 10 mM MOPS, pH 7.0, were mixed with 20 mM dithionite in the same buffer at 25 °C. The percent change in the steady-state velocity was determined by dividing the experimental steady-state velocity (*27*) by that for the unmodified control and multiplying by 100.

Kinetics of DBDS Release from Band 3 As Measured by the Decrease in Fluorescence Associated with Replacement of DBDS by DIDS. Unsealed ghosts were prepared from control or from the various modified erythrocytes and washed in 300 mM sodium gluconate, 20 mM Bistris, and 20 mM Tris, pH 7.4. The concentration of ghosts was adjusted so that all samples had the same concentration of total membrane protein, to which DBDS was added from a 6.5 mM stock solution in water to yield a final concentration of 6.24 μM. Solutions containing various mixtures of chloride and gluconate were prepared in the Bistris/Tris buffer by mixing 300 mM sodium gluconate with 300 mM sodium chloride in various ratios, so as to maintain constant ionic strength. DIDS was added to these latter solutions from an 18 mM stock solution in water to yield a concentration of 13 μM. The reaction was initiated by mixing equal volumes of the DBDS/membrane complex with the DIDS-containing solutions at 25 °C in a Gibson-Durrum stopped-flow apparatus. The decrease in fluorescence associated with the release of DBDS (*18*) was followed by excitation at 335 nm, with observation through a 415 nm cutoff filter. Under these conditions there was no contribution to the fluorescence change from reversible binding of DIDS (*20*) or from the formation of the covalent adduct between DIDS and lysine A (*24*), owing to the very much slower rate of this latter reaction as compared to the rate of the DBDS/DIDS replacement reaction (see below). Ten reactions, each consisting of 1000 data points, were signal averaged for any given reaction condition.

Kinetics of DBDS Binding to Band 3. The kinetics of DBDS binding were followed under pseudo-first-order ligand binding conditions in the stopped-flow apparatus as described in our previous report (*28*). The reactions for control and

WRKB-modified membranes were studied as a function of DBDS concentration between 2 and 10 μM in 150 mM NaCl, 20 mM Bistris, and 20 mM Tris, pH 7.4, at 25 °C. The increase in DBDS fluorescence was observed by excitation at 335 nm, with observation through a 415 nm cutoff filter. The biphasic time courses were analyzed by fitting the data to a function representing the sum of two exponentials (*28*). Initial second-order rate constants for DBDS binding were determined (*28*).

Data Analysis. Kinetic data were analyzed quantitatively using Sigma Plot (SPSS Science, Chicago, IL). Primary digital data from the stopped-flow data acquisition system (OLIS, Athens, GA) were imported into the Sigma Plot program as ASCII files for direct analysis. The kinetic data were fitted to either single or double exponential functions. Secondary plots were also fitted using Sigma Plot according to the equations described in the legends to the figures.

RESULTS

Kinetics of DBDS Release from Control Band 3. We have investigated the chloride-binding properties of band 3 using our highly sensitive DBDS "off" rate method (*18*−*21*). Release of DBDS from a complex with band 3, by replacement with DIDS, is followed by making observations through a 415 nm cutoff filter, with the excitation wavelength set at 335 nm. Replacement is associated with a decrease in DBDS fluorescence. The rate of this reaction is limited by the release of DBDS, and the reaction is considered to be essentially irreversible owing to the extremely slow off rate for reversibly bound DIDS (see theoretical considerations and experimental tests given in ref *18*). We have shown that chloride and other monovalent substrate anions bind rapidly to the exofacially oriented transport site (*18*, *19*), within the DBDS/band 3 binary complex, and accelerate DBDS release allosterically (*18*−*21*). The time course for this reaction is always monophasic and exponential when membranes containing unmodified, wild-type band 3 are used (Figure 1A). Mixing DBDS bound to membranes in gluconate with DIDS in solutions containing various chloride and gluconate mixtures at constant ionic strength caused an hyperbolic increase in the DBDS off rate constant, with an apparent K_d of 259 ± 37 mM, a k_{max} of 3.4 ± 0.3 s^{-1}, and a k_{min} of 0.18 ± 0.01 s^{-1} (Figure 1B). We have found that treatment of intact cells with sodium borohydride alone, under the same conditions as used in the experiments described below, did not change the behavior of control band 3. Furthermore, acceleration in DBDS release is specific for monovalent substrate anions, since divalent substrate anions (sulfate) and so-called "spectator" anions, such as citrate and gluconate, do not accelerate the rate of DBDS release beyond a weak ~2-fold effect seen when ionic strength is allowed to vary over a wide range (*18*, *19*). Finally, we show, in the insert to Figure 1B, that the absolute value of the fluorescence change for the DBDS/DIDS reaction does not vary with increasing chloride. Thus, the effect of chloride is to increase the rate of DBDS release allosteically without changing the fluorescent spectral characteristics of the reaction. This finding agrees with all of our previous studies using chloride and the various other monovalent substrate anions, all of which accelerate the rate of DBDS release (*18*, *19*).

Characteristics of the Transport and DIDS Covalent Binding Properties of Erythrocytes Modified by the Various Woodward's Reagent K/Borohydride Treatment Strategies. Jennings and co-workers (*12*, *13*) have shown that modification of band 3 with Woodward's reagent K/borohydride leads to inhibition of monovalent anion exchange and to activation of divalent/monovalent anion transport, which is inhibited by H_2DIDS. We have used a novel SCN^-/Cl^- exchange assay published in an earlier report from our laboratory (*23*) to measure the rate of monovalent anion exchange across the erythrocyte membrane. Figure 2A shows the effect of modifying membranes with the various types of WRKB treatments used in this study. We find that the various treatments can be ranked with respect to the degree of inhibition of monovalent anion exchange as follows: control < WRKB < 2(WRKB) < (2WRK + B), with these specific treatments defined in the Experimental Procedures section. This ranking agrees completely with the findings of Jennings

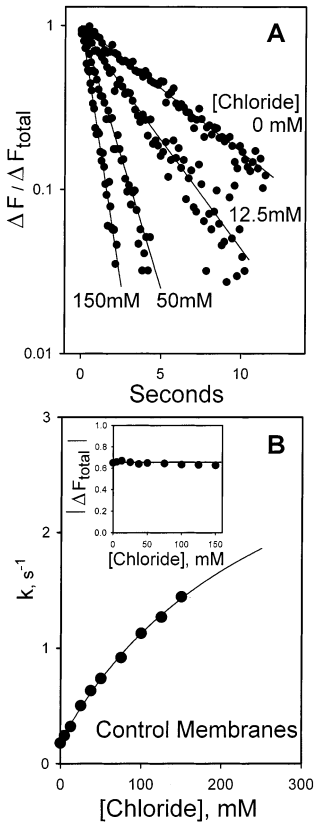

FIGURE 1: Effect of chloride on the DBDS off rate for unmodified control unsealed ghosts as measured by the DBDS/DIDS replacement reaction (*18*, *19*). Unsealed ghosts were prepared, and total membrane protein was determined as described in the Experimental Procedures section of the text. Ghosts were in 300 mM sodium gluconate, 20 mM Bistris, and 20 mM Tris, pH 7.4. DBDS was added to give 6.25 μM before the mix. This sample was mixed with 13 μM DIDS in either the same gluconate buffer (zero chloride condition) or in buffer containing various sodium gluconate/sodium chloride ratios at constant ionic strength equivalent to 300 mM. (A) Normalized time course for the replacement reaction. The rate constants at each chloride concentration were 0 mM = 0.18 ± 0.01 s^{-1}, 12.5 mM = 0.32 ± 0.002 s^{-1}, 50 mM = 0.74 ± 0.01 s^{-1}, and 150 mM = 1.45 ± 0.01 s^{-1}. (B) Plot of the observed rate constants versus chloride concentration. The data were fit to an equation of the form described by Fersht (*36*): $k = (k_{max}[\text{chloride}] + K_d k_{min})/(K_d + [\text{chloride}])$. The values of the constants are k_{max} = 3.4 ± 0.3 s^{-1}, k_{min} = 0.18 ± 0.01 s^{-1}, and K_d = 259 ± 37 mM. The insert shows a plot of the change in total fluorescence for the DBDS/DIDS replacement reaction measured at the various chloride concentrations for the same membrane preparation.

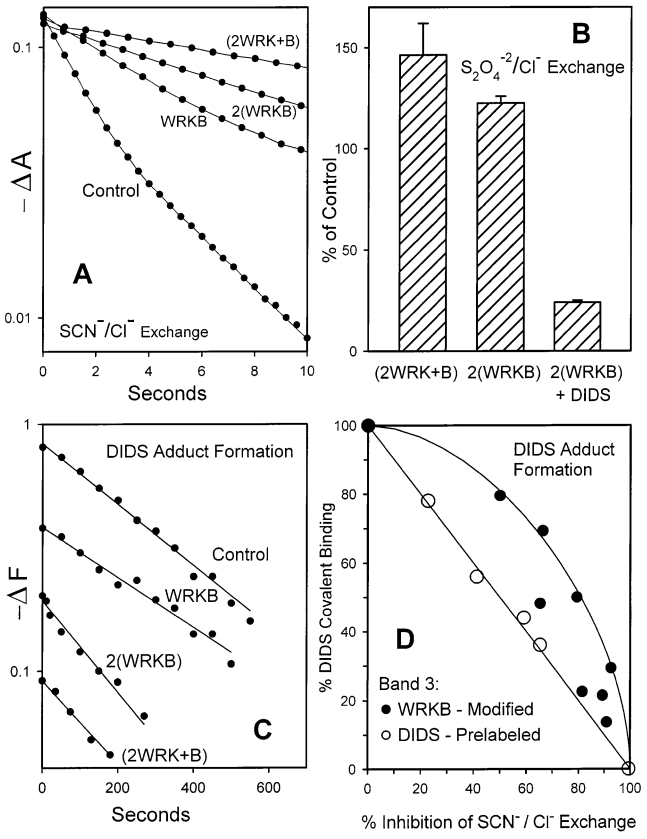

FIGURE 2: Various assays for the transport function of band 3 and for lysine A reactivity toward covalent binding of DIDS, all of which were measured as a function of various Woodward's reagent K/sodium borohydride (WRKB) treatments. (A) Thiocynate (SCN^-)/chloride (Cl^-) exchange in intact erythrocytes followed by observing the change in intracellular methemoglobin absorbance upon reaction with SCN^- (*23*). The absorbance change is presented as $(-1)(\Delta A)$, so as to present that change as a decreasing function of time. Initial rates were calculated (*23*), and the percent inhibition of transport was determined: control = 0%; WRKB (i.e., one WRKB treatment cycle) = 66%; 2(WRKB) (two WRKB treatment cycles) = 82%, and (2WRK + B) (two treatments with WRK followed by borohydride) = 91%. See the Experimental Procedures section for complete details on the various WRKB methods. (B) Dithionite ($S_2O_4^{2-}$)/Cl^- exchange measurements (*26*, *27*) for the various WRKB-modified intact erythrocytes. The transport of this divalent anion increased by 147 ± 16% for cells treated with (2WRK + B), compared to control (not shown), and it increased by 123 ± 4% for 2(WRKB)-modified cells. Addition of 6.5 μM DIDS to the 2(WRKB)-modified cells inhibited dithionite influx to 24 ± 1% of control flux. The error bars represent standard errors for experiments using two independent cell preparations from different individuals. (C) Plot of the time course for the change in fluorescence associated with formation of the DIDS covalent adduct with lysine A (*24*). The fluorescence change is presented as $(-1)(\Delta F)$, so as to present that change as a decreasing function of time. The reactions were made with matching ghosts in 300 mM sodium gluconate, 20 mM Bistris, and 20 mM Tris, pH 7.4, at 25 °C. (D) Correlation plots of the percent DIDS covalent binding to reactive band 3 versus the percent inhibition of SCN^-/Cl^- exchange. The closed circles represent data from membranes from two different individuals whose cells were reacted with various Woodward's reagent K/borohydride modification strategies to yield different levels of SCN^-/Cl^- transport inhibition (Figure 2A). Open circles were measured for control membranes prelabeled with an increasing fraction of covalent binding of DIDS as described in the Experimental Procedures section. SCN^-/Cl^- exchange activity was determined on the intact cells, and the fraction of DIDS-reactive subunits was determined on the respective unsealed ghost preparations as described above. The line through the control data points is the 1:1 correlation line. The curve drawn through the data from membranes modified with different Woodward's reagent K strategies (closed circles) was calculated on the basis of the statistical dimer model, where only dimers with both subunits modified lose their capacity to react with DIDS (see text and legend to Figure 5C for further details).

and co-workers (*12*, *13*, *22*). Furthermore, such modification of band 3 subunits leads to activation of divalent anion/chloride exchange, which is inhibitable by DIDS (Figure 2B). We see that the (2WRK + B) treatment activates divalent anion transport to a somewhat greater degree than does 2(WRKB) treatment (Figure 2B). This corresponds to the greater degree of subunit modification and agrees with the findings of Jennings (*22*). We did not see as large an activation of divalent anion transport using dithionite, as was seen by Jennings et al. (*12*, *13*, *22*), who used sulfate. This is most likely related to the fact that dithionite transport is about 10-fold faster than sulfate transport in unmodified erythrocytes (*29*), yet both types of transport activity are probably accelerated to approximately the same maximum by modification of band 3.

We suspected that fractional inhibition of SCN^-/Cl^- exchange by treatment with Woodward's reagent K/borohydride corresponded to the fractional modification of band 3 subunits. We used the ability of DIDS to react with lysine A (*1*, *24*) to test this hypothesis. DIDS binds reversibly to native band 3, with a 1:1 subunit stoichiometry (*20*), and then reacts to make a covalent adduct with lysine A (*1*). Adduct formation is linked allosterically to the state of the transport site (*1*). Adduct formation can be followed quantitatively by measuring the change in fluorescence (excitation 360 nm, emission 450 nm) upon formation of the covalent adduct (*24*). Therefore, DIDS can be used to titrate active band 3 subunits quantitatively.

Figure 2C shows the kinetics of fluorescence change associated with covalent binding of DIDS to lysine A for control and for the various types of modified membranes. Membrane concentrations were matched exactly for all samples (*25*). There was a substantial diminution in the extent of the DIDS reaction for these samples. The kinetic reactions were carried to completion (not shown) so that ΔF_{total} values could be compared. In Figure 2D, the percent of DIDS covalent binding was then correlated with the percent inhibition of SCN^-/Cl^- exchange for each modification strategy. Both measurements were performed on the same preparation. Each of the closed circles in Figure 2D represents a different modified sample. It is apparent that the correlation plot does not follow the 1:1 correlation line. There appeared to be more DIDS-reactive band 3 subunits than would have been predicted on the basis of the percent inhibition of SCN^-/Cl^- exchange.

The implication of the nonlinear correlation plot in Figure 2D (closed circles) is that modification with Woodward's reagent K/borohydride leads to a population of band 3 subunits which are incapable of exchanging SCN^-/Cl^- but are capable of forming a covalent bond between DIDS and lysine A. However, this interpretation requires that we establish that the SCN^-/Cl^- exchange activity is a property of a single band 3 subunit. Such a linear correlation has been demonstrated for chloride self-exchange (*1*, *3*) and even for dithionite/sulfate exchange (*30*). Although we had shown that SCN^-/Cl^- exchange activity was inhibited totally by covalent binding of DIDS (*23*), we did not determine whether inhibition of transport activity and DIDS labeling were correlated linearly. To accomplish this, we labeled erythrocytes with various amounts of DIDS and measured SCN^-/Cl^- exchange. We then isolated the membranes and measured covalent binding of DIDS to unreacted subunits using our

fluorescence assay for covalent bond formation with lysine A (*24*). Figure 2D (open circles) shows that there is a linear relationship between the band 3 subunit population which is reactive toward DIDS and those subunits which are capable of performing SCN^-/Cl^- exchange. Thus, SCN^-/Cl^- exchange is a function of individual band 3 subunits. The nonlinear correlation seen in Figure 2D (closed circles) cannot be ascribed to some type of anomaly associated with SCN^-/Cl^- exchange assay per se. The curved line in Figure 2D was calculated as will be described below.

Chloride-Induced Development of 50:50 Biphasic Kinetics for DBDS Release from Band 3 Treated with Various Woodward's Reagent K/Borohydride Strategies. The normalized time course for DBDS release was monophasic and exponential in the absence of chloride (Figure 3A), both for control and for (2WRK + B)-modified membranes [91% inhibition of monovalent anion exchange (Figure 2A)]. This level of modification slowed the rate of DBDS release by 46% (Figure 3A, open circles). Using a less stringent modification strategy (WRKB) [resulting in 66% inhibition of monovalent anion exchange (Figure 2A)], the DBDS release rate was slowed by 17% while remaining monophasic and exponential (Figure 3B, 0 mM chloride).

When modified membranes were mixed with chloride at constant ionic strength such that 75 mM chloride was present after mixing, the time course for the DBDS/DIDS replacement reaction became ~50:50 biphasic (Figure 3B, 75 mM). One-half of the band 3 subunits released DBDS about 6 times faster than the slow-release half. We note that similar rapid mixing experiments of WRKB-modified membranes with sulfate (45 mM after the mix) did not accelerate DBDS release, despite the fact that chloride and sulfate are both substrates of band 3 (*1*−*3*, *29*).

Chloride-Induced Development of a 50:50 Biphasic Kinetic Time Course Is Associated with a Large Increase in the Fluorescence Quantum Yield of DBDS Molecules Bound to Modified Band 3. The effect of chloride on the fluorescence of DBDS bound to modified band 3 was investigated as a function of the degree of modification by the Woodward's reagent K/borohydride treatment between ~66% and 91% inhibition of SCN^-/Cl^- exchange (Figure 4A−I). In these experiments, membranes were prepared, and transport and DIDS covalent binding characteristics were determined as described in the Experimental Procedures section. The spectral−kinetic behavior of the DBDS/DIDS replacement reaction is shown for each modification in three-panel sets (A−C, D−F, and G−I). For each set of figures, a given membrane preparation was suspended in the DBDS/gluconate buffer and mixed in the stopped-flow apparatus with constant DIDS in various chloride/gluconate mixtures so as to maintain constant ionic strength. Thus, any observed difference in fluorescence amplitude reflects a difference in the fluorescence of bound DBDS molecules (a) since the membrane concentration was constant, (b) since the concentration of inhibitors is always the same, and (c) since the ionic strength never changes. In addition, the membrane protein concentrations for the three sets of modification strategies used in Figures 4 were matched on an absolute basis (described in Experimental Procedures). This allows the fluorescence amplitudes to be compared directly between sets in Figure 4 [i.e., WRKB (A−C) versus 2(WRKB) (D, E) versus (2WRK + B) (G−I)].

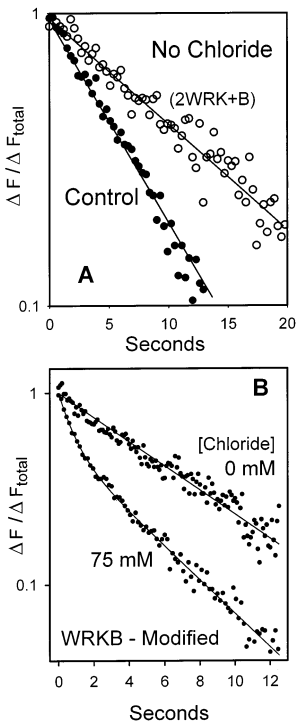

FIGURE 3: DBDS/DIDS replacement reaction for unmodified control band 3 and for band 3 modified by treatment with Woodward's reagent K/borohydride. (A) No chloride. The DBDS/DIDS replacement reaction was measured in 300 mM sodium gluconate and 20 mM Bistris, plus 20 mM Tris, pH 7.4, 25 °C. DBDS was added to unsealed ghosts to give 6.25 μM before the mix. This sample was mixed with 13 μM DIDS in the same gluconate buffer. Two samples of unsealed ghosts were used, i.e., unmodified control and (2WRK + B)-modified. The SCN^-/Cl^- exchange rate was inhibited by 91% for (2WRK + B)-modified membranes compared to control. The DBDS/DIDS replacement rate constant for control band 3 was 0.18 ± 0.01 s^{-1}. The rate constant for (2WRK + B)-modified band 3 was 0.082 ± 0.001 s^{-1}, a 46% reduction in the rate of DBDS release. There was no evidence for kinetic heterogeneity for (2WRK + B) membranes measured in the absence of chloride. (B) Effect of chloride on the kinetics of DBDS release from modified band 3. DBDS was added to ghosts in the 300 mM sodium gluconate buffer described above to give 6.25 μM before the mix. This sample was mixed with 13 μM DIDS in either the same gluconate buffer or a buffer containing 150 mM sodium gluconate/150 mM sodium chloride before the mix. The unsealed ghosts were derived from erythrocytes which had been modified using the WRKB strategy (Experimental Procedures). The SCN^-/Cl^- exchange rate was inhibited for these WRKB-modified membranes by 66% compared to control. The time course for the DBDS/DIDS replacement reaction measured for WRKB membranes in the absence of chloride followed monophasic, exponential kinetics with an apparent rate constant of $k = 0.15 \pm 0.001$ s^{-1} (~17% inhibition compared to the unmodified control). The time course for the 75 mM chloride condition was biphasic and was fit to a double exponential equation after normalizing the change in the fluorescence signal: $\Delta F/\Delta F_{total} = a \exp(-k_{fast}t) + b \exp(-k_{slow}t)$, with $a = 0.46 \pm 0.01$, $k_{fast} = 1.21 \pm 0.04$ s^{-1}, $b = 0.53 \pm 0.01$, and $k_{slow} = 0.2 \pm 0.003$ s^{-1}.

We were surprised to find that rapid mixing with chloride induced the development of a 2-fold increase in the fluorescence quantum yield of the DBDS molecules bound to the various types of modified band 3 preparations. Such a chloride-induced change in fluorescence is never seen for control band 3 under otherwise identical conditions (Figure 1B). WRKB-modified membranes (66% inhibition of SCN^-/Cl^- exchange) showed a monophasic DBDS/DIDS replacement reaction time course in the absence of chloride (Figure

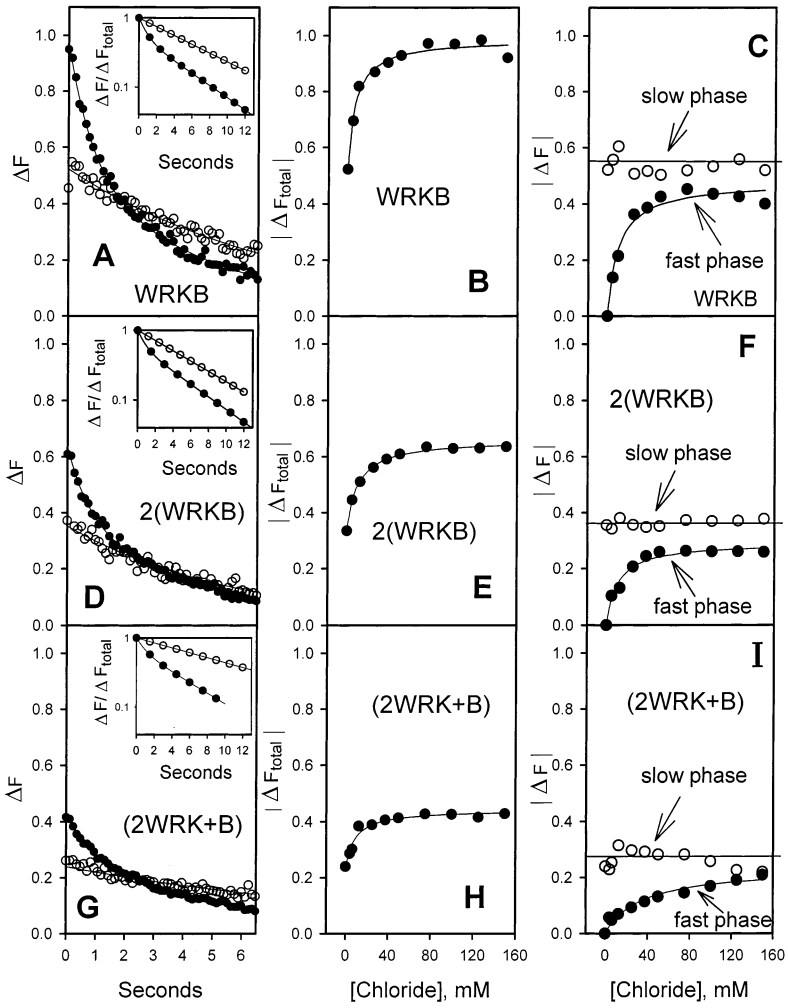

FIGURE 4: Effect of chloride on the time course and amplitude of the fluorescence change for the DBDS/DIDS replacement reaction using unsealed ghosts derived from erythrocytes treated with the various Woodward's reagent K/borohydride strategies (Experimental Procedures). In all of these experiments intact erythrocytes were modified and unsealed ghosts prepared and matched for total membrane protein as described in the Experimental Procedures section. Ghosts were in 300 mM sodium gluconate, 20 mM Bistris, and 20 mM Tris, pH 7.4. DBDS was added to give 6.25 μM before the mix. This sample was mixed with 13 μM DIDS in 20 mM Bistris and 20 mM Tris, pH 7.4, containing 150 mM sodium gluconate and 150 mM sodium chloride (before the mix) for panels A, D, and G, or the ghosts were mixed with various sodium chloride and sodium gluconate solutions so as to vary chloride concentration while maintaining constant ionic strength (panels B, E, H, C, F, and I). In each panel, the points are the data and the lines are the corresponding fitted results, except for the inserts in A, D, and G, where points and lines come from the fits. Note that, in contrast to Figure 3, the results presented here do not use normalized changes in the fluorescence signal. (A) Time course for the DBDS/DIDS reaction using unsealed ghosts derived from WRKB-modified erythrocytes. The time course for the reaction measured in the absence of chloride (open circles) gave a good fit to a single exponential function of the form $\Delta F = \Delta F_0 \exp(-kt)$, where $\Delta F_0 = 0.524 \pm 0.005$ and $k = 0.15 \pm 0.001$ s^{-1}. The time course for the reaction measured in the presence of chloride (closed circles) gave a good fit to an equation representing the sum of two exponentials, $\Delta F = \Delta F_f \exp(-k_f t) + \Delta F_s \exp(-k_s t)$, where $\Delta F_f = 0.45 \pm 0.001$, $k_f = 1.21 \pm 0.04$ s^{-1}, $\Delta F_s = 0.52 \pm 0.01$, and $k_s = 0.2 \pm 0.003$ s^{-1}. The insert shows a semilog plot of the fitted curves for each data set normalized to their respective ΔF_{total} values. (B) Plot of the chloride dependence of the absolute value of ΔF_{total} for the DBDS/DIDS reaction using unsealed ghosts derived from WRKB-modified erythrocytes. The data gave a good fit to a function of the form $\Delta F_{total} = \Delta F^0_{total} + \{(\Delta F_m[Cl^-])/(K_d + [Cl^-])\}$, with $\Delta F^0_{total} = 0.52 \pm 0.03$, $\Delta F_m = 0.47 \pm 0.03$, and $K_d = 7.2 \pm 1.6$ mM. (C) Plot of the chloride dependence of the preexponential factors for the DBDS/DIDS replacement reaction using unsealed ghosts derived from WRKB-modified erythrocytes. The fast-phase amplitudes gave a good fit to a simple hyperbolic function of the form $\Delta F = (\Delta F_m[Cl^-])/(K_d + [Cl^-])$, with $\Delta F_m = 0.48 \pm 0.02$ and $K_d = 10.2 \pm 1.9$ mM. (D) Time course for the DBDS/DIDS reaction using unsealed ghosts derived from 2(WRKB)-modified erythrocytes. The time course for the reaction measured in the absence of chloride (open circles) gave a good fit to a single exponential function of the form $\Delta F = \Delta F_0 \exp(-kt)$, where $\Delta F_0 = 0.37 \pm 0.003$ and $k = 0.13 \pm 0.02$ s^{-1}. The time course for the reaction measured in the presence of chloride (closed circles) gave a good fit to an equation representing the sum of two exponentials, $\Delta F = \Delta F_f \exp(-k_f t) + \Delta F_s \exp(-k_s t)$, with $\Delta F_f = 0.26 \pm 0.01$, $k_f = 1.26 \pm 0.05$ s^{-1}, $\Delta F_s = 0.37 \pm 0.01$, and $k_s = 0.21 \pm 0.003$ s^{-1}. The insert shows a semilog plot of the fitted curves for each data set. (E) Plot of the chloride dependence of the absolute value of ΔF_{total} for the DBDS/DIDS reaction using unsealed ghosts derived from 2(WRKB)-modified erythrocytes. The data gave a good fit to a function of the form $\Delta F = \Delta F^0_{total} + \{(\Delta F_m[Cl^-])/(K_d + [Cl^-])\}$, with $\Delta F^0_{total} = 0.35 \pm 0.01$, $\Delta F_m = 0.33 \pm 0.01$, and $K_d = 10.2 \pm 0.8$ mM. (F) Plot of the chloride dependence of the preexponential factors for the DBDS/DIDS replacement reaction using unsealed ghosts derived from 2(WRKB)-modified erythrocytes. The fast-phase amplitudes gave a good fit to a simple hyperbolic function of the form $\Delta F = (\Delta F_m[Cl^-])/(K_d + [Cl^-])$, with $\Delta F_m = 0.29 \pm 0.01$ and $K_d = 10.5 \pm 1.9$ mM. (G) Time course for the DBDS/DIDS reaction using unsealed ghosts derived from (2WRKB + B)-modified erythrocytes. The time course for the reaction measured in the absence of chloride (open circles) gave a good fit to a single exponential function of the form $\Delta F = \Delta F_0 \exp(-kt)$, where $\Delta F_0 = 0.24 \pm 0.001$ and $k = 0.082 \pm 0.001$ s^{-1}. The time course for the reaction measured in the presence of chloride (closed circles) gave a good fit to an equation representing the sum of two exponentials, $\Delta F = \Delta F_f \exp(-k_f t) + \Delta F_s \exp(-k_s t)$, where $\Delta F_f = 0.15 \pm 0.004$, $k_f = 1.07 \pm 0.05$ s^{-1}, $\Delta F_s = 0.28 \pm 0.004$, and $k_s = 0.18 \pm 0.003$ s^{-1}. (H) Plot of the chloride dependence of the absolute value of ΔF_{total} for the DBDS/DIDS reaction using unsealed ghosts derived from (2WRKB + B)-modified erythrocytes. The data gave a good fit to a function of the form $\Delta F = \Delta F^0_{total} + \{(\Delta F_m[Cl^-])/(K_d + [Cl^-])\}$, with $\Delta F^0_{total} = 0.23 \pm 0.02$, $\Delta F_m = 0.21 \pm 0.02$, and $K_d = 8.8 \pm 2.2$ mM. (I) Plot of the chloride dependence of the preexponential factors for the DBDS/DIDS replacement reaction using unsealed ghosts derived from (2WRKB + B)-modified erythrocytes. The fast-phase amplitudes gave a good fit to a simple hyperbolic function of the form $\Delta F = (\Delta F_m[Cl^-])/(K_d + [Cl^-])$, with $\Delta F_m = 0.24 \pm 0.02$ and $K_d = 34.7 \pm 9$ mM.

4A and insert, open circles). However, the amplitude for the change in reaction fluorescence was about one-half of that seen when the very same membrane suspension was mixed with an isoionic chloride/gluconate solution, such that the final chloride concentration was 75 mM (Figure 4A, closed circles). The insert in Figure 4A and the analysis given in the legend to that figure show that the reaction becomes ~50:50 biphasic upon addition of chloride. Furthermore, the amplitude of the reaction fluorescence change can be titrated as a function of chloride concentration (Figure 4B). Such a titration yields a saturation curve that follows a hyperbolic function with a nonzero intercept and gives an apparent K_d value of 7 mM for chloride binding. It is apparent from the results in Figure 4B that the amplitude of the reaction increases almost 2-fold compared to the amplitude of the reaction measured in the absence of chloride.

We next fitted each time course measured in the presence of chloride to a double exponential function of the form given in the legend to Figure 4. Kinetic constants were extracted and amplitudes for the fast (ΔF_{fast}) and for the slow (ΔF_{slow}) phases determined as a function of chloride concentration. Figure 4C shows a plot these amplitudes versus chloride concentration. It is clear that the amplitude of the slow DBDS release phase (Figure 4C, open circles) does not change with increasing chloride. All of the increase in fluorescence amplitude (Figure 4B) arises from the chloride-induced formation of the fast DBDS release phase (Figure 4 C, closed circles). The effect of chloride on the kinetic constants will be described below.

Panels D−F of Figure 4 show the same experiment for 2(WRKB)-modified membranes. In this case, intact erythrocytes were modified with two cycles of WRKB treatment, which consistently resulted in ~82% inhibition of SCN^-/Cl^- exchange (Figure 1A). It is apparent from inspection of Figure 4D that the general findings seen at the lower level of subunit modification remained the same. Addition of chloride increased the amplitude of the reaction fluorescence about 2-fold. The increase was dependent on chloride in a saturable fashion (Figure 4E), with an apparent K_d of about 10 mM. Once again, all of the chloride-induced change in fluorescence arose from the fluorescence properties of the fast phase (Figure 4F). However, there was one very significant difference between the results in Figure 4D−F, compared to Figure 4A−C. Increasing the degree of modification resulted in a marked diminution in the amplitude for the total change in fluorescence, despite the fact that the membrane concentrations were matched exactly.

To investigate the effect of even higher degrees of modification by Woodward's reagent K/borohydride treatment, we treated cells with (2WRK + B) using the method of Jennings (*22*). This modification gave 91% inhibition of SCN^-/Cl^- exchange (Figure 2A). In Figure 4G−I, we see that the general characteristics for the effect of chloride on the kinetics of DBDS release from (2WRK + B)-modified membranes were the same as seen in the other panels in Figure 4 at lower modification levels. Biphasic kinetics were induced by chloride. This change is associated with a near doubling in the amplitude of the total fluorescence change for the DBDS/DIDS replacement reaction (Figure 4G). The K_d associated with the increase in total reaction fluorescence was about 9 mM (Figure 4H). The increase in fluorescence arose from the fast phase (Figure 4I). However, the size of the total change in fluorescence was even lower for (2WRK + B)-modified membranes, despite the fact that we used membrane concentrations that were matched exactly.

Correlation Plots for the Total Change in Fluorescence for the DBDS/DIDS Replacement Reaction Versus the Degree of Band 3 Subunit Modification by Treatment with Woodward's Reagent K/Borohydride. The series of experiments shown in Figure 4 demonstrates clearly that the 50:50 biphasicity induced by chloride does not simply reflect the populations of modified and unmodified band 3 subunits. Figure 5 summarizes the effect of band 3 modification on the total change in fluorescence for the DBDS/DIDS replacement reaction. In Figure 5A, we plot the ΔF_{total} for the DBDS/DIDS replacement reaction as a percent of ΔF_{total} for matching unmodified control membranes (e.g., Figure 1B, insert) for a given series of modification strategies. This ratio is plotted versus the percent of modified band 3 subunits. Modification of subunits is taken as the percent inhibition of SCN^-/Cl^- exchange for the same cells from which the membranes were derived. The data shown in Figure 5A were from experiments performed in the absence (Figure 5A, curve 3, closed circles) and in the presence (Figure 5A, curve 4, open circles) of saturating amounts of chloride. If there were a 1:1 correlation between subunit modification and reversible binding of DBDS, one would expect a linear correlation plot (line 1 in Figure 5A). Instead, a nonlinear decrease is seen in the absence of chloride, and the data go through a maximum in the presence of chloride.

Figure 5A, curve 2, is from Figure 2D for DIDS covalent binding to various modified membranes, plotted as a function of the percent modification of band 3 subunits. The DBDS data measured in the absence of chloride (closed circles) do not fall on curve 2. This point is confirmed in Figure 5B, where ΔF_{total} for the DBDS/DIDS replacement reaction as a percent of ΔF_{total} for matching unmodified control is plotted versus the percent DIDS covalent binding (Figure 2D) for the various respective modified membranes. A nonlinear relationship was observed, indicating that the DBDS fluorescence change is sensitive to different factors in the modified preparation, as compared to the direct measure of the fraction of DIDS-reactive subunits. For example, in Figure 5B, at 50% binding of DIDS, more than 50% binding of DBDS is indicated on the basis of the change in reaction fluorescence relative to unmodified control. However, such a difference is never observed for unmodified control band 3. The insert to Figure 5B is data reproduced from our earlier publication (*18*) showing that, for control band 3, there is a perfectly linear relationship between the change in fluorescence associated with reversible binding of DBDS and the fractional covalent binding of DIDS.

We performed an experiment to test for the unlikely possibility that there is a fluorescence change associated with the binding of DIDS, which may contribute to the observed change in the total fluorescence for the DBDS/DIDS replacement reaction. We investigated DBDS binding in "forward-flow" kinetic experiments for modified membranes (66% inhibition of SCN^-/Cl^- exchange) measured in the presence of 150 mM chloride (Figure 5A, the point marked by the X). The ratio of amplitudes for the change in fluorescence for binding of DBDS to modified and unmodified band 3 in the absence of DIDS was essentially the same as that seen for the DBDS/DIDS replacement reaction. Thus, we can

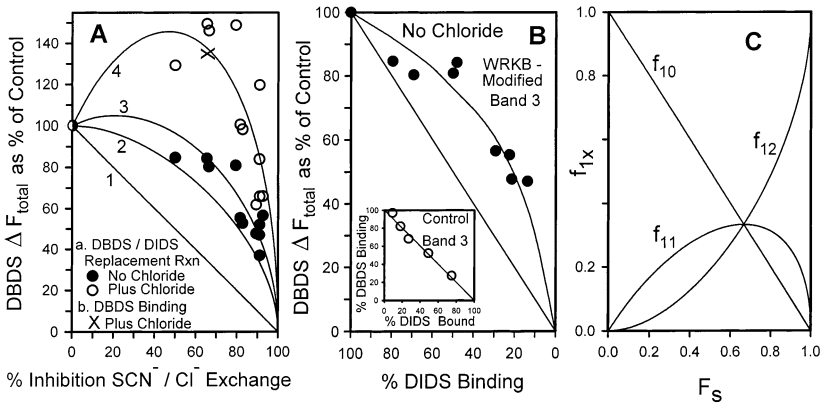

FIGURE 5: (A) ΔF_{total} for the DBDS/DIDS replacement reaction for unsealed ghosts presented as a percent of ΔF_{total} for unmodified control membranes (e.g., Figure 1B, insert) plotted versus the percent of subunits modified by treatment with Woodward's reagent K/borohydride. Percent modification was taken to be equal to the percent inhibition of SCN^-/Cl^- exchange. Measurements were made in the absence (closed circles) or in the presence (open circles) of saturating chloride concentration (>75 mM). These data were derived from the unmodified control, WRKB-modified cells (at various concentrations of reagent), and 2(WRKB)- and (2WRK + B)-modified cells treated as described in the Experimental Procedures section. These data were obtained from six independent experiments using erythrocytes from six different anonymous donors drawn by the Omaha Chapter of the American Red Cross. The X represents a ΔF_{total} measurement for DBDS binding in forward flow (i.e., the DBDS kinetic "on" experiment), measured in the presence of 150 mM NaCl, 20 mM Bistris, and 20 mM Tris, pH 7.4. Line 1 is the 1:1 correlation line. Curve 2 was calculated on the basis of the dimer model (see Figure 5C and the text for details). Curves 3 and 4 were drawn on the basis of similar model calculations. (B) Plot of ΔF_{total} for the DBDS/DIDS replacement reaction as a percent of ΔF_{total} for matching unmodified control membranes versus the percent DIDS binding to reactive band 3 subunits. Each point represents membranes treated with a different modification strategy. The straight line is the 1:1 correlation line. The curved line through the data is drawn by hand and has no specific theoretical significance. The insert shows a plot of the percent DBDS binding, at saturating DBDS concentration, versus the percent of DIDS covalently bound. Band 3 was treated with DIDS prior to mixing with DBDS. DBDS binding was determined by the change in fluorescence upon mixing with DBDS in the forward-flow kinetic "on" experiment. The data used in this insert were taken from Figure 2B of our earlier publication (*18*) and are presented here for ease in making comparisons with the data for membranes modified by treatment with Woodward's reagent K/borohydride. (C) Plot of the fraction of dimeric molecular species for subunit modification in a noncooperative dimer model. The *y*-axis is the fraction of the given species f_{1x}, where f_{10} = unmodified dimer, f_{11} = dimer with one modified subunit, and f_{12} = fully modified dimer. These fractions were calculated according to a theory (*31*), where modification of subunits is noncooperative and where each subunit has the same Woodward's reagent K initial binding constant. The values of f_{10}, f_{11}, and f_{12} were used to calculate values of the *x*- and *y*-axes of correlation plots such as those in Figures 2D and 5A. For the *x*-axis we calculate a sorting function F_s, defining the fraction of dimers on which one or more subunits are modified. Thus, $F_s = f_{11} + f_{12}$. If we assume that stilbenedisulfonates do not bind to the fully modified dimer, then fractional stilbenedisulfonate binding will be equal to $1 - f_{12}$, which will be a decreasing function of F_s after an initial lag (i.e., the inverse of the curve marked f_{12}). Such a theoretical curve is plotted for the DIDS binding data of Figure 2D and as curve 2 in Figure 5A. If we assume that only half-modified dimers possess an altered fluorescence quantum yield for bound DBDS molecules, one can calculate a new *y*-axis term. Let the fraction of species which bind DBDS be defined as $y' = f_{10} + f_{11}(1 + \alpha)$. Thus, when $\alpha = 0$, $y' = f_{10} + f_{11} = 1 - f_{12}$. This defines the DIDS binding curve of Figure 2D and curve 2 in Figure 5A. When the half-modified intermediate has a different fluorescence quantum yield, then $\alpha > 0$ and $f_{10} + f_{11}(1 + \alpha) > f_{10} + f_{11}$. This defines curves 3 and 4 in Figure 5A, where $\alpha = 0.5$ was used to calculate curve 3 and $\alpha = 2.09$ was used to calculate curve 4.

assign the change in fluorescence amplitude in the DBDS/DIDS replacement reaction to a rapid, chloride-induced, change in the fluorescence quantum yield of DBDS molecules bound to modified band 3.

Calculation of the Fraction of Dimeric Molecular Species Present as a Function of the Degree of Modification of the Band 3 Subunit Population: Application to the Problem of Nonlinear Correlation Plots for Stilbenedisulfonate Binding versus Band 3 Subunit Modification. In this section we develop a model to rationalize the nonlinear correlation plots seen for covalent binding of DIDS (Figure 2D, closed circles) and for reversible binding of DBDS (Figure 5A) measured in the absence and presence of chloride. To understand these patterns, it is critical to calculate the various dimeric molecular species expected at any given level of fractional modification of band 3 subunits. The method used for calculation of the fraction of species present for a two-site, dimer model has been described elsewhere (*31*). Figure 5C shows a plot of the fraction of the three types of dimeric molecular species expected to be populated along such a modification manifold. The fractions were calculated on the assumption that band 3 exists as a stable dimer in the erythrocyte membrane (*32*−*35*) and that subunit modification by treatment with Woodward's reagent K/borohydride is a noncooperative process (*22*) involving reversible, independent binding of the reagent to each unmodified subunit prior to the modification reaction.

The calculated values shown in Figure 5C were generated for the fraction of molecular species, f_{1x} ($x = 0-2$), where f_{10} = the unmodified dimer; f_{11} = the half-modified dimer, and f_{12} = the fully modified dimer. These values are plotted against the term F_s, which is a "sorting function" (*31*) used to distinguish unmodified dimers from the two types of modified dimers (i.e., $F_s = f_{11} + f_{12}$). F_s has values ranging from 0 to 1. We consider this term to be equivalent to the fractional inhibition of monovalent anion transport activity by band 3 subunits, since we showed that the percent inhibition of SCN^-/Cl^- exchange is linearly related to modification of subunits by DIDS (Figure 2D, open circles). DIDS is known to bind to band 3 with a 1:1 subunit stoichiometry (*20*). In Figure 5C, it is clear that the unmodified dimer disappears in a linear fashion as the half-modified and fully modified dimers are formed. The half-modified dimer appears and disappears as an intermediate,

while the fully modified dimer appears after a lag and is the final species present when all subunits in the population are modified (see legend to Figure 5C for further details).

We propose that nonlinear correlation plots of the type seen in Figures 2D and 5A can be rationalized by suggesting that each dimeric molecular species generated along the modification manifold has different properties with respect to (a) the ability of the various species to bind stilbenedisulfonates, (b) the spectral characteristics measured in the absence of chloride for those species which do bind stilbenedisulfonates, and (c) the spectroscopic response of the various complexes to the rapid addition of chloride. From the plots in Figure 5C, it seems that one can describe the loss in DIDS and DBDS binding capacity by simply relating such change to the appearance of the fully modified dimer, if it is assumed that that species does not bind stilbenedisulfonates. The curve in Figure 2D and curve 2 in Figure 5A were generated on the assumption that covalent binding of DIDS takes place within unmodified band 3 dimers and within both subunits of half-modified band 3 dimers but not within the subunits of the fully modified dimer. In other words, covalent binding of DIDS is allowed for the modified subunit within the half-modified dimer but not to modified subunits within the fully modified dimer. This stipulation is necessary or the correlation plot would be linear, and it is not.

The data for reversible binding of DBDS in the absence of chloride (Figure 5A, closed circles) clearly reflect the same type of loss in binding capacity that was seen for covalent binding of DIDS (Figure 2D). Yet, there was a lack of correlation between DBDS and DIDS for data where both measurements were made on the same cells (Figure 5B). We have assumed that this failure to correlate occurs for the same reason that such a failure occurs when chloride is added (Figure 5A, open circles). We propose that deviations from correlation curves generated by the simple dimer model are the consequence of an increased fluorescence quantum yield for the intermediate, half-modified dimeric molecular species. We can calculate the *y*-axis given in Figure 5A by using the equation *y*-axis value $= 100(1 + \alpha f_{11} - f_{12}) = 100[f_{10} + f_{11}(1 + \alpha)]$, since $1 = f_{10} + f_{11} + f_{12}$. This *y*-axis term is an alternate sorting function which calculates the fraction of "not fully modified band 3 dimer". The equation accounts for the larger fluorescence quantum yield of the intermediate DBDS/half-modified dimer complex and for the fact that the signal is lost as the fully modified dimer forms. Thus, when $\alpha > 0$, the *y*-axis value will exceed 100% during transient formation of the half-modified dimer. But as f_{10} approaches zero and f_{11} goes through a maximum and then approaches zero (Figure 5C), the value of the above *y*-axis term will approach zero, to reflect the increased fraction of the fully modified band 3 dimer, f_{12}, which, in our model, does not bind DBDS or DIDS. We generated curves 3 and 4 in Figure 5A using a value for α of 0.5 to calculate curve 3 (no chloride) and using a value for α of 2.09 to calculate curve 4 (saturating chloride). We conclude that the dimer model, as just outlined, is consistent with all of the stilbenedisulfonate binding data for band 3 subunits modified by Woodward's reagent K/borohydride treatment of intact erythrocytes (*12*, *13*, *22*).

The Dependence of the Kinetic Constants for DBDS Release on Chloride Concentration Suggests the Presence of Two Classes of Chloride-Binding Sites on Modified Band 3. Figure 6 shows the kinetic constants from the fits of the various experiments with WRKB-, 2(WRKB)-, and (2WRK + B)-modified membranes as a function of chloride concentration (closed circles in each panel). We placed the results from Figure 1B, for unmodified control band 3, into each panel of Figure 6 (open circles) to make direct comparisons easier. It is apparent that the chloride dependence of the rate constants was not hyperbolic for band 3 modified by the Woodward's reagent K/borohydride method. We see a lag instead of the uniform increase in the rate constant as seen with control. The lag persists up to a chloride concentration of about 60 mM for both fast and slow phases regardless of the modification strategy employed. This is the same concentration range over which chloride induces the increase in fluorescence for DBDS/band 3 complexes (Figure 4B,E,H). Further increases in the concentration of chloride caused the rate constants to increase for both fast and slow

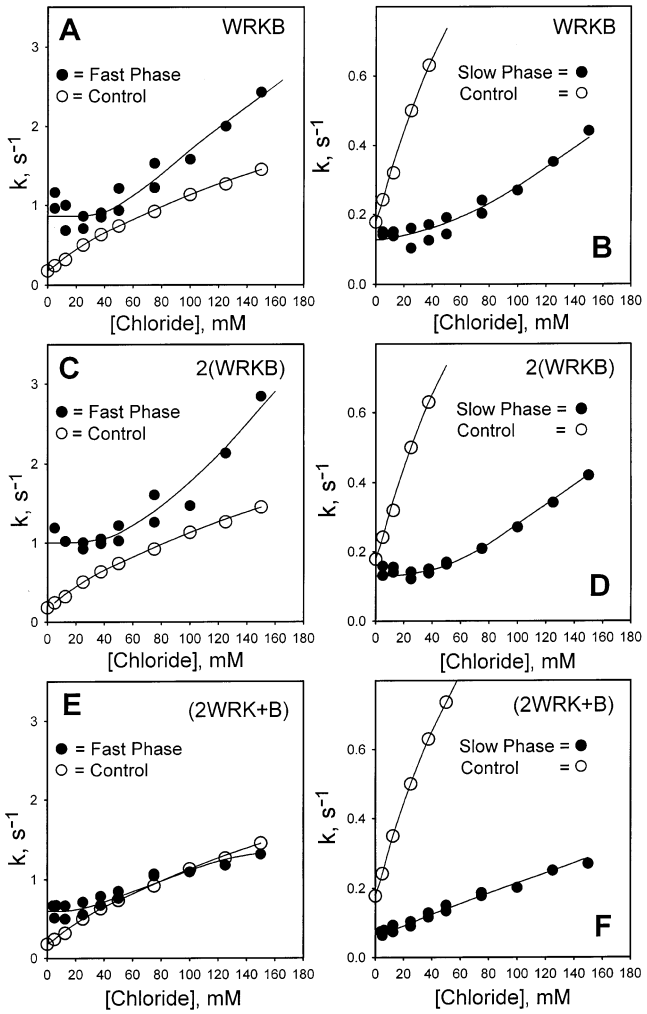

FIGURE 6: Effect of chloride on the fast- and slow-phase rate constants for the DBDS/DIDS replacement reaction. The rate constants were obtained from two independent erythrocyte preparations. The control data were reproduced from Figure 1B to allow for direct comparison. The curves through the data (closed circles) were drawn by hand. The curve through the control was drawn on the basis of a fit to a hyperbolic function as described in the legend to Figure 1. Panels A and B: unsealed ghosts derived from WRKB-modified erythrocytes. Panels C and D: unsealed ghosts derived from 2(WRKB)-modified erythrocytes. Panels E and F: unsealed ghosts derived from (2WRK + B)-modified erythrocytes.

phases (Figure 6). This increase occurred over a range similar to that responsible for the increase in rate constant for the control and is consistent with chloride binding to the transport site (Figure 1B) (*18*, *19*). However, it is noted that the response of the slow-phase rate constant to increasing chloride is highly attenuated when compared to unmodified control band 3. We conclude that the nonhyperbolic behavior of the DBDS off rate constants is consistent with the presence of two classes of chloride-binding sites on modified band 3.

Effect of Chloride on the Initial Rate Constants for DBDS Binding to Band 3 in Membranes Derived from Control and WRKB-Modified Erythrocytes. We have also measured the DBDS "on" rate constants (*28*) for control and for WRKB-modified band 3 (66% inhibition of SCN^-/Cl^- exchange) and found no significant difference in the initial rate of DBDS binding measured in 150 mM chloride, 20 mM Bistris, and 20 mM Tris, pH 7.4, at 25 °C. The values of the kinetic constants associated with the first step in the two-step reversible binding mechanism for stilbenedisulfonate binding to band 3 (*20*, *28*) were as follows: for control membranes, $k_1 = (1.0 \pm 0.3) \times 10^6\ M^{-1}\ s^{-1}$ and $k_{-1} = 9.0 \pm 3.0\ s^{-1}$, and for WRKB-modified membranes, $k_1 = (1.4 \pm 0.3) \times 10^6\ M^{-1}\ s^{-1}$ and $k_{-1} = 11.0 \pm 3.0\ s^{-1}$. The lack of effect of modification on the on kinetic constants in the presence of chloride suggests that the net effect of modification by Woodward's reagent K/borohydride is reflected in the DBDS off rate constant. Thus, when chloride is present, the affinity of stilbenedisulfonate for one subunit becomes ~6-fold lower than the affinity of its neighbor.

DISCUSSION

Development of Spectral and Kinetic Heterogeneity in Band 3 Modified by Treatment of Cells with Woodward's Reagent K/Borohydride Is Related to the Formation of the Half-Modified Band 3 Dimer. The key to understanding the complex spectral−kinetic data presented in this report is to consider the distribution of molecular species which are present as a function of the degree of modification of the band 3 subunit population, using a two-subunit (one site per subunit), noncooperative dimer modification model. This model seems applicable to Woodward's reagent K/borohydride modification of band 3 in intact erythrocytes. First, band 3 exists in situ as stable dimers (*32*−*35*) [which can associate to tetramers (dimer of dimer) upon interaction with ankyrin]. Native monomers could not be detected within intact membranes, while in situ unfolding of the membrane domain of band 3 did yield denatured monomers (*35*). Woodward's reagent K/borohydride modifies a single glutamate (glutamate 681) as established by Jennings and Smith (*13*). Finally, this modification process showed no evidence for cooperativity of either a negative or positive type (22).

At each fractional degree in the overall modification process, the fraction of the three types of dimers can be determined (Figure 5C). The fraction of each species is plotted versus the sum of the fractions of modified species (F_s). Modification of membranes with the so-called WRKB strategy (defined in Experimental Procedures) reproducibly modified about 66% of subunits on the basis of the loss of SCN^-/Cl^- exchange activity (Figure 2A), which we take as the percent modification of the band 3 subunit population. Thus, with 66% of the subunits modified, the calculations in Figure 5C indicate that each dimeric species will represent approximately 33% of the species present. Similarly, 2(WRKB) modifies about 82% of the subunits, with about 50% doubly modified, 30% singularly modified, and 20% unmodified dimers. Finally, (2WRK + B) modifies 91% of the subunits, and this mixture would contain 9% unmodified, 25% singularly modified, and 66% doubly modified dimers. Once the distribution of dimeric species is established, it is then necessary to consider the properties of each dimeric species with respect to (a) the ability to bind stilbenedisulfonates, (b) the spectral and kinetic characteristics for the bound stilbenedisulfonate in the absence of chloride, and (c) the spectral and kinetic response of such band 3 dimer/stilbenedisulfonate complexes to the rapid addition of chloride.

The characteristics observed for the unmodified band 3 dimer in the DBDS/DIDS replacement reaction are relatively simple (*18*). First, the replacement reaction always shows monophasic and exponential kinetics (*18*). Second, rapid addition of chloride or other monovalent substrate anions (*19*) accelerates the rate of release in a manner consistent with binding to a single, low-affinity class of sites, identified as the transport site within the DBDS/band 3 binary complex (*18*−*20*). Third, the rapid addition of chloride, while greatly accelerating the rate of DBDS release, has no effect on the fluorescence quantum yield of the reaction (Figure 1B, insert).

In Figure 4, the two prominent features of the data are (a) the dramatic loss of total fluorescence signal with increased level of modification and (b) the equally dramatic response of the fluorescence signal and the kinetics to the addition of chloride. We propose that the increase in the fraction of doubly modified dimer most likely accounts for the dramatic loss in signal. This view is supported by the observation of grossly nonlinear correlation plots in Figure 2D for DIDS binding and in Figure 5A for DBDS binding, both plotted as a function of the percent inhibition of SCN^-/Cl^- exchange activity. To confirm that this loss in signal corresponds to the appearance of the doubly modified dimer, we calculated the fraction of this species for the DIDS binding data, where no potential complications from changes in DIDS fluorescence need be considered (see Results). The curve in Figure 2D gave a good representation of the data (closed circles).

The results in Figure 5 showed that, when measured in the absence of chloride (closed circles), the DBDS data behaved in a qualitatively similar, but quantitatively different manner as compared to the pattern observed for covalent binding of DIDS shown in Figure 2D. The DBDS data (closed circles) deviated from the correlation curve established for DIDS (Figure 5A curve 2), which more closely followed the expectations from theoretical calculations of the fraction of unreactive subunits contained within the fully modified band 3 dimer (Figure 5C). This difference was evident in Figure 5B. We suggest that the reason for this difference is that DBDS bound to half-modified dimers has a slightly enhanced fluorescence quantum yield as compared to control, even in the absence of chloride. Calculations were given in Results that support this interpretation. Thus, simply forming the half-modified band 3 dimer must generate a different conformational state as compared to unmodified band 3 and the fully modified dimer which does not bind stilbenedisulfonates.

The need for a more complex modification scheme is seen most clearly for the DBDS/DIDS reaction for modified band 3 performed in the presence of saturating chloride concentration (Figure 5A, open circles, curve 4). It is evident that the data go though a maximum. This behavior can be interpreted empirically as follows. Initially, unmodified subunits are present which do not show the chloride-induced change in fluorescence (insert to Figure 1B). Then an apparent "intermediate" species develops as modification by the various Woodward's reagent K/borohydride strategies yield increased levels of modified band 3 subunits. The DBDS fluorescence quantum yield for this intermediate undergoes a large increase upon addition of chloride (Figure 4). Finally, treatment with Woodward's reagent K/borohydride to yield higher levels of band 3 subunit modification results in a transporter which does not bind DBDS or DIDS (Figures 2D, 4, and 5). The entire signal nearly disappears for the binding of these inhibitors.

These impressions were quantitatively supported by the calculations which generated the shape of curve 4 in Figure 5A, as described in the Results section and in the legend to Figure 5C. This curve reflects the increase in fluorescence quantum yield for DBDS bound to modified band 3 in the presence of chloride. This is a characteristic of the half-modified band 3 dimer population only. Therefore, this remarkable signal change is a consequence of the appearance and disappearance of the half-modified band 3 dimeric intermediate species formed during the overall modification process. It is the only species which binds DBDS that is capable of such a response. Unmodified band 3 does not change its fluorescence spectrum (Figure 1B), while fully modified band 3 dimer does not bind DBDS (Figures 4 and 5).

It is mechanistically important to consider the contribution of each reaction phase to the large increase in the total fluorescence quantum yield (Figure 4BE,H). This can be accomplished by performing quantitative analysis of the amplitudes of the two phases of the reaction as a function of chloride concentration (Figure 4C,F,I). The chloride-induced increase in fluorescence quantum yield was associated with the development of 50:50 biphasic kinetics for DBDS release. One-half of the fluorescence change is apportioned to the "fast-release subunits" and the other half to the "slow release subunits" (Figure 4). All of the chloride-induced increase in fluorescence arises from the fast-release subunits. There is no change in the amplitude for the slow-release subunits (Figure 4C,F,I). Moreover, the absolute value of the amplitude for the slow-release subunit is the same as the amplitude for all subunits measured in the absence of chloride.

Two explanations for such behavior can be envisioned. One is that one-half of the modified band 3 subunits are cryptic stilbenedisulfonate sites, which are "recruited" to the outer surface of the membrane upon addition of saturating amounts of chloride. However, we would not expect to observe such a "recruitment" of band 3 subunits in the type of kinetic experiment performed in Figure 4. This is because any new stilbenedisulfonate site would be occupied immediately by the excess DIDS present in the reaction mixture, since the higher concentration and extreme tight binding of DIDS would offer substantial competition to DBDS binding. Indeed, it is this property of DIDS which forms the basis for our DBDS/DIDS replacement reaction (*18*).

We propose a second, more likely explanation for asymmetric behavior of the amplitudes for each kinetic phase in the DBDS release reaction. We suggest that the addition of saturating amounts of chloride rapidly converts a preexisting, DBDS-bound, half-modified band 3 dimer to an asymmetric state where one-half of the subunits are fast-release subunits and the other half are slow and where the increase in the fluorescence amplitude occurs for DBDS bound to both fast-release and slow-release subunits. The net result would be a conversion of one-half of the slow-release subunits to fast-release subunits but a compensating 2-fold increase in fluorescence quantum yield of the slow release subunit, resulting in no change in the fluorescence amplitude of the slow-release subunits, while the total fluorescence would double. These considerations suggest that chloride changes the conformation of the entire half-modified band 3 dimer from a structurally symmetrical conformational state to a highly asymmetrical conformational state.

Evidence for the Existence of Two Chloride-Binding Sites in the Half-Modified Band 3 Dimer, One the Low-Affinity Transport Site and the Other the Cryptic Modifier Site Which Has ~40 Higher Affinity. The results of this paper support the hypothesis that glutamate 681 interacts with a high-affinity, conformationally active chloride-binding modifier site. Modification with Woodward's reagent K/borohydride of only one subunit on a dimer of band 3 neutralizes (*12*) the charge on glutamate 681, specifically (*13*), and exposes a cryptic chloride-binding site. Chloride binding to this site produces a 2-fold increase in the fluorescence quantum yield of DBDS molecules bound to modified band 3 (Figure 4B,E,H). Titration of the chloride-induced increase in fluorescence yielded an apparent K_d of 7−10 mM. This value contrasts with the apparent K_d of 259 mM for the chloride dependence of the DBDS release rate constant for unmodified band 3 (Figure 1B). Our previous work, using several monovalent substrate anions, identified this low-affinity site as the transport site within the DBDS/band 3 binary complex (*19*).

The kinetic constants for the half-modified band 3 dimer show several complexities that support the two chloride-binding site hypothesis. In the absence of chloride, DBDS release from the subunits of the half-modified band 3 dimer is uniform (monophasic, exponential kinetics; Figure 3A), but the rate is slower because of a proposed structural change in the entire dimer. Such a structural change in the entire dimer is suggested by the slightly altered DBDS fluorescence (Figure 5A, curve 3, closed circles, modified band 3 with no chloride). Rapid mixing with chloride converts the DBDS-bound half-modified dimer from a symmetrical conformational state to an asymmetrical conformational state, leading to a doubling in the DBDS fluorescence and acceleration in the rate of DBDS release from one of the subunits and an attenuated chloride-induced alteration in the slow-release subunit (Figure 6).

The nonhyperbolic dependence of the apparent rate constants on chloride concentration, for both the fast and slow phases (Figure 6), offers strong evidence for the existence of two classes of chloride-binding sites. The lag occurs over the same concentration range as the titration of fluorescence signal in Figure 4. The implication is that when

the fast phase is observed, it has a given fast off rate constant, which does not change with increasing chloride. Thus, one simply generates more of that state up to saturation (Figure 4), but the rate constants of that state are otherwise insensitive to chloride binding to the modifier site. After that initial lag, the rate constants for both phases of the modified protein show the low-affinity acceleration of the rate constant, which is assigned to chloride binding to the transport site.

How Does the Dimer Model Used To Rationalize the Data of This Paper Relate to the Monovalent and Divalent Transport Activity of Band 3? Jennings and co-workers (*12*, *13*, *22*) found, and we have confirmed (Figure 2A,B), that modification of band 3 subunits with Woodward's reagent K/borohydride leads not only to the complete inhibition of monovalent anion exchange but also to the activation of divalent anion transport in exchange for chloride. Activation of divalent transport was inhibitable by H_2DIDS (*12*, *13*, *22*), and we find that DIDS also inhibits divalent transport activity in modified cells (Figure 2B). Yet, it is clear that DIDS and DBDS (and presumably H_2DIDS) do not bind to the subunits within the fully modified dimer, as indicated by the loss in DBDS fluorescence signal with increased modification (Figures 4 and 5) and the nonlinear correlation plot for DIDS binding (Figure 2D). The dimer model proposes that the unmodified dimer and both subunits of the half-modified dimer bind DBDS and DIDS. Thus, inhibition by DIDS, of all but the last ~24% of divalent transport activity (Figure 2B), suggests that such remaining activity should be assigned to the doubly modified fraction of the band 3 dimer, since this species does not bind DIDS. 2(WRKB) samples had ~82% of subunits modified (Figure 2A). The model calculations in Figure 5C indicate that at 82% modification of band 3 subunits there should be ~50% doubly modified dimers, 30% half-modified dimers, and 20% unmodified dimers. Thus, our experimental observation of ~24% DIDS-refractory transport activity is half as much activity as would have been expected. While the doubly modified dimer does appear to contain transport-active subunits, their "turnover number" may be smaller than unmodified band 3. Mechanistically, such a reduction could be due to a 2-fold lower activity, with the subunit as the functional unit or alternatively, the dimer is the functional unit for divalent anion transport (*27*). Nevertheless, it seems to follow that all three types of dimeric molecular species (unmodified, half-modified, and fully modified dimers) are transport active.

We have assigned the function of the allosteric regulatory modifier site which appears after neutralization of the negative charge on glutamate 681 to be one which facilitates the anion/proton cotransport process. It is possible that this site is involved in transport, but there is no evidence to that effect. We propose that the carboxyl side chain of glutamate 681 interacts with the high-affinity chloride-binding modifier site. Lowering the pH would protonate the carboxyl, causing it to dissociate from its "docking site", which in turn would allow for chloride binding to the high-affinity site and to the conversion of the transporter from the symmetrical dimeric state to the asymmetrical dimeric state. This conversion is proposed to be associated with the inhibition of monovalent anion exchange and with the activation of divalent (sulfate) proton cotransport. Having chloride bound to the glutamate docking site should facilitate proton transport by preventing the "redocking" of the negatively charged side chain of glutamate 681. The consequence would be to raise the p*K* of glutamate 681, thus allowing it to pick up a proton for the cotransport process.

The existence of a high-affinity monovalent anion binding site, where chloride and the protein-bound glutamate carboxyl compete, may explain the puzzling characteristic of band 3 known as "self-inhibition" (*1*−*4*). Competition between solution chloride and the carboxyl side chain of glutamate 681 for binding to the modifier site could potentially account for the observation of self-inhibition, if such chloride binding converts the band 3 dimer from a symmetrical conformational state which actively exchanges monovalent anions to an asymmetrical conformational state where that activity is inhibited. Since the side chain of glutamate 681 is bound to the protein, it would have a very large thermodynamic advantage in competition with solution chloride. This would require that very high chloride concentrations be used to displace the glutamate side chain and produce self-inhibition. Such behavior is consistent with observation (*1*−*4*).

In summary, our results present the first spectral and kinetic evidence for the existence of an apparent high-affinity, chloride-binding, allosteric modifier site, which functions to convert band 3 from a symmetrical to an asymmetrical dimeric conformational state. We have suggested that the function of this site is to facilitate the anion/proton cotransport function of band 3.

ACKNOWLEDGMENT

We thank Dr. L. M. Schopfer for discussions and for reading a draft of the manuscript, Dr. M. L. Jennings for discussions and suggestions on procedures for modification of band 3 by Woodward's reagent K and sodium borohydride, and Mr. M. Mercer for discussions.

REFERENCES

1. Passow, H. (1986) *Rev. Physiol. Biochem. Pharmacol. 103*, 61−223.
2. Salhany, J. M. (1990) *Erythrocyte Band 3 Protein*, CRC Press, Boca Raton, FL.
3. Jennings, M. L. (1992) Anion Transport Proteins, in *The Kidney*: *Physiology and Pathophysiology* (Seldin, D. W., and Giebisch, G., Eds.) pp 113−145, Raven Press, New York.
4. Knauf, P. A. (1979) *Curr. Top. Membr. Transp. 12*, 249−363.
5. Weith, J. O., and Brahm, J. (1985) Cellular anion transport, in *The Kidney*: *Physiology and Pathophysiology* (Seldin, D. W., and Giebisch, G., Eds.) pp 49−89, Raven Press, New York.
6. Milanick, M. A., and Gunn, R. B. (1982) *J. Gen. Physiol. 79*, 87−113.
7. Jennings, M. L. (1976) *J. Membr. Biol. 28*, 187−205.
8. Milanick, M. A., and Gunn, R. B. (1984) *Am. J. Physiol. 247*, C247−C259.
9. Gunn, R. B. (1972) A titratable carrier model for both mono- and di-valent anion transport in human red blood cells, in *Oxygen Affinity of Hemoglobin and Red Cell Acid*−*Base Status* (Rorth, M., and Astrup, P., Eds.) pp 823−827, Munksgaard, Copenhagen.
10. Jennings, M. L. (1978) *J. Membr. Biol. 40*, 365−391.
11. Passow, H., Lepke, S., and Heberle, J. (2001) *Biophys. J. 80*, 46a−46a.
12. Jennings, M. L., and Al-Rhaiyel, S. (1988) *J. Gen. Physiol. 92*, 161−178.
13. Jennings, M. L., and Smith, J. S. (1992) *J. Biol. Chem. 267*, 13964−13971.
14. Chernova, M. N., Jiang, L., Crest, M., Hand, M., Vandorpe, D. H., Strange, K., and Alper, S. L. (1997) *J. Gen. Physiol. 109*, 345−360.
15. Sekler, I., Lo, R. S., and Kopito, R. R. (1995) *J. Biol. Chem. 270*, 28751−28758.

16. Dutzler, R., Campbell, E. B., Cadene, M., Chait, B. T., and MacKinnon, R. (2002) *Nature 415*, 287−294.
17. Bahar, S., Gunter, C. T., Wu, C., Kennedy, S. D., and Knauf, P. A. (1999) *Am. J. Physiol. 277*, C791−C799.
18. Salhany, J. M., Sloan, R. L., Cordes, K. A., and Schopfer, L. M. (1994) *Biochemistry 33*, 11909−11916.
19. Salhany, J. M. (1999) *Biochem. Cell Biol. 77*, 543−549.
20. Salhany, J. M. (1996) *Cell. Mol. Biol. 42*, 1065−1096.
21. Salhany, J. M. (2001) *Blood Cells, Mol. Dis. 27*, 901−912.
22. Jennings, M. L. (1995) *J. Gen. Physiol. 105*, 21−47.
23. Salhany, J. M. (1998) *Biochem. Mol. Biol. Int. 45*, 181−190.
24. Schopfer, L. M., and Salhany, J. M. (1995) *Biochemistry 34*, 8320−8329.
25. Salhany, J. M., Sloan, R. L., and Cordes, K. A. (1990) *J. Biol. Chem. 265*, 17688−17693.
26. Salhany, J. M., and Swanson, J. C. (1978) *Biochemistry 17*, 3354−3362.
27. Salhany, J. M., and Crodes, K. A. (1992) *Biochemistry 31*, 7301−7310.
28. Salhany, J. M., Sloan, R. L., Cordes, K. A, and Schopfer, L. M. (1995) *Int. J. Biochem. Cell Biol. 27*, 953−964.
29. Jennings, M. L. (1989) *Annu. Rev. Biophys. Biophys. Chem 18*, 397−430.
30. Salhany, J. M., and Rauenbuehler, P. B. (1987) *J. Biol. Chem. 262*, 15974−15978.
31. Conners, K. A. (1987) *Binding Constants. Measurement of Molecular Complex Stability*, pp 21−101, John Wiley and Sons, New York.
32. Yu, J., and Steck, T. L. (1975) *J. Biol. Chem. 250*, 9170−9175.
33. Wang, D. N., Sarabia, V. E., Reithmeier, R. A. F., and Kuhlbrandt, W. (1994) *EMBO J. 13*, 3230−3235.
34. Salhany, J. M., Cordes, K. A., and Sloan, R. L. (1997) *Mol. Membr. Biol. 14*, 71−79.
35. Salhany, J. M., Cordes, K. A., and Sloan, R. L. (2000) *Biochem. J. 345*, 33−41.
36. Fersht, A. (1977) *Enzyme Structure and Mechanism*, pp 134−137, W. H. Freeman, San Francisco.

BI0205294